Electronic Supplementary Material (ESI) for Journal of Materials Chemistry

Supplementary Information

Pure and mixed gas adsorption of CH_4 and N_2 on the metal-organic framework Basolite® A100 and a novel copper-based *1,2,4*-triazolyl benzoate MOF

Jens Möllmer[(1)], Marcus Lange[(1)], Andreas Möller[(1)], Christin Patzschke[(1)], Karo Stein[(1)], Daniel Lässig[(2)], Jörg Lincke[(2)], Roger Gläser[(1)], Harald Krautscheid[(2)] and Reiner Staudt[(3)]*

[1] *Institut für Nichtklassische Chemie e.V. Permoserstr. 15, D-04318 Leipzig, Germany*
E-Mail: moeller@inc.uni-leipzig.de
[2] *Universität Leipzig, Fakultät für Chemie und Mineralogie, Johannisallee 29, D-04103 Leipzig, Germany*
E-Mail: krautscheid@rz.uni-leipzig.de
[3] *Hochschule Offenburg, Fakultät Maschinenbau und Verfahrenstechnik, Badstraße 24, D-77652 Offenburg*
E-Mail: Reiner.Staudt@fh-offenburg.de

1 Characterisation of adsorbents by N_2 adsorption at 77 K

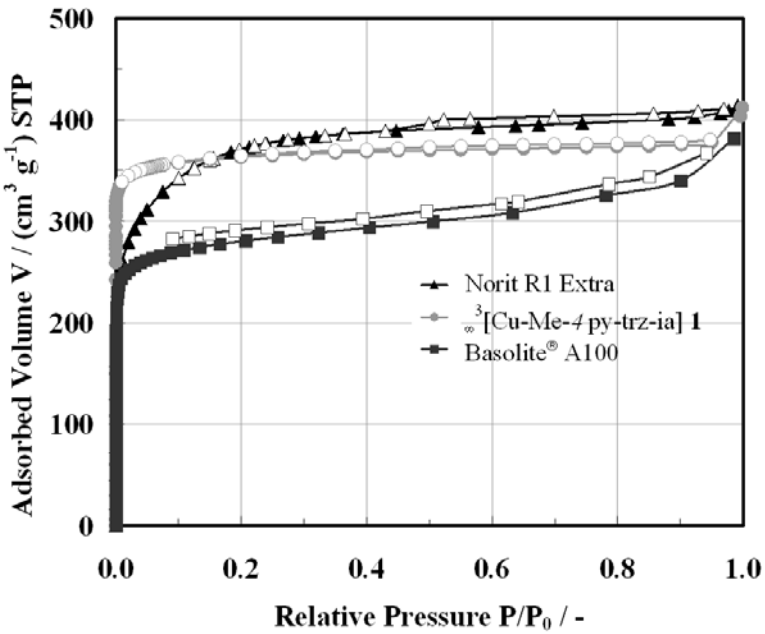

Fig. SI1 N_2 adsorption and desorption isotherms at 77 K on Basolite® A100, $_\infty^3$[Cu(Me-*4*py-trz-ia)] **1** and Norit R1 Extra; closed symbols: adsorption and open symbols: desorption, lines are to guide the eyes.

.

Tab. SI1 Textural properties of adsorbents calculated from N_2 adsorption isotherm.

Adsorbent	Textural properties from experimental N_2 adsorption isotherm			
	BET[(a)] / $m^2\ g^{-1}$	$V_{Pore,\ total}$[(b)] / $cm^3\ g^{-1}$	$V_{Pore,\ micro}$[(c)] / $cm^3\ g^{-1}$	d[(d)] / nm
Basolite® A100	1085[(e)]	0.492	0.463	6.2
$_\infty^3$[Cu(Me-*4*py-trz-ia)] **1**	1473	0.586	0.585	5.5
Norit R1 Extra	1332	0.636	0.611	5.4

(a) BET-method for microporous solids according to reference.[1-3]
(b) total pore volume calculated by Gurvich-rule at $P/P_0 = 0.9$.[4,5]
(c) micropore volume calculated by Dubinin-Astakhov-method.[5]
(d) Average pore diameter d from NLDFT approach.
(e) Customer value 1100 -1500 $m^2\ g^{-1}$.[6]

2 Powder X-ray diffraction

The PXRD measurements were carried out on a STOE STADI-P diffractometer in Debye-Scherrer mode using Cu-$K_{\alpha1}$ radiation ($\lambda = 154.060$ pm). The samples for these measurements were prepared in capillaries (outer diameter 0.5 mm).

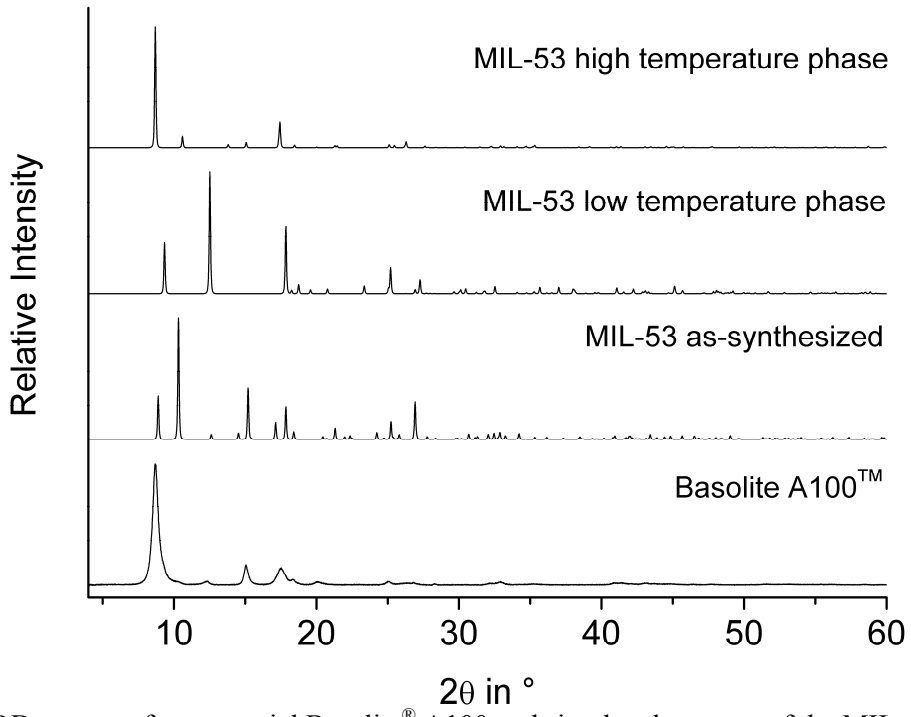

Fig. SI2 XRD pattern of commercial Basolite® A100 and simulated patterns of the MIL-53 series[7].

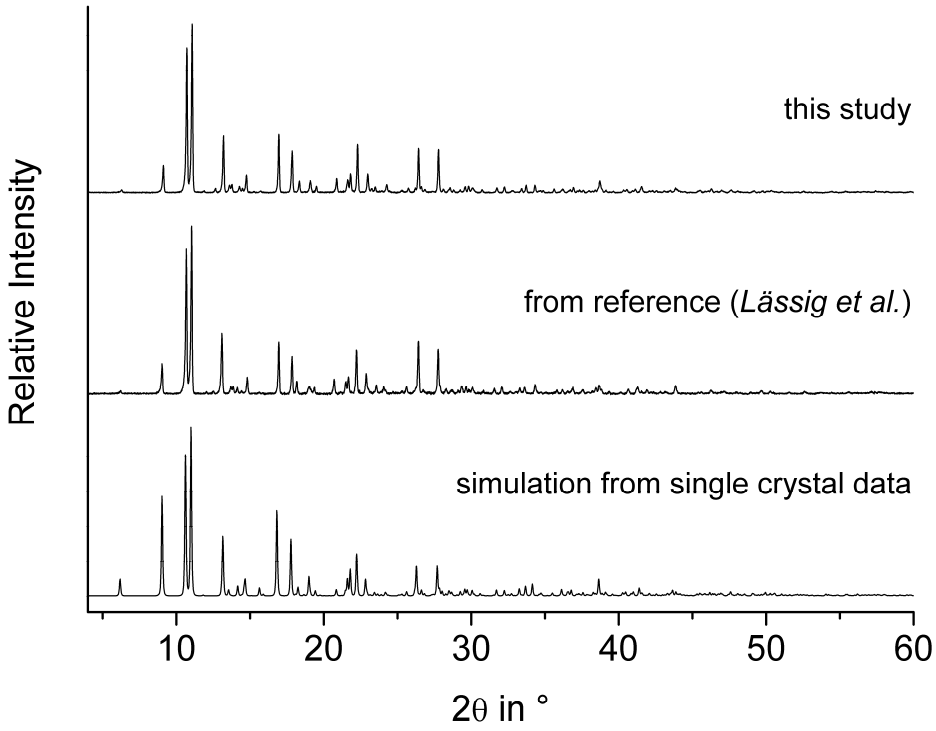

Fig. SI3 Experimental and simulated XRD powder patterns of $^{3}_{\infty}$[Cu(Me-*4*py-trz-ia)] **1**.[8]

3 Theory

3.1 Models for describing pure gas adsorption

Tòth model

To describe the adsorption isotherm over a wide range of pressure it is important to use a model that has several essential characteristics.[9] One is the thermodynamical applicability to the chosen adsorbent-adsorbate system, another one is the quality of the data description by the usage of this model.[9] Therefore, we use the Tòth isotherm model[9,10] and the *vacancy solution model* and applying the Wilson equation[10,11] for the description of the pure gas isotherms. In the following, it will be shown that both models can be used to predict binary adsorption.[10,12,13]

The Tòth isotherm equation was developed to describe the influence of a heterogeneous surface on the slope and the shape of the adsorption isotherms.[9] Therefore, the Tòth isotherm model can be seen as the enhancement of the Langmuir isotherm model.[9] From the three parameter Tòth isotherm equation

$$\theta = \frac{n}{n_{max}} = \frac{b \cdot p}{(1 + (b \cdot p)^t)^{1/t}}, \qquad (1)$$

it is obvious that the parameter t represents the heterogeneity of the adsorbent-adsorbate system. If the parameter t is equal to 1 the Tòth isotherm equation is equivalent to the

Langmuir isotherm equation. Furthermore, the Henry's law constant H_T of the Tòth isotherm equation can be calculated by

$$\mathbf{H_T = n_{max} \cdot b}. \qquad (2)$$

Vacancy solution model

The *vacancy solution model* (VSM) was developed by Suwanayuen and Danner in 1980.[11] It describes the adsorption regarding two phases, the gas phase and the adsorbed phase. Both differ tremendously in their densities and can be considered as a solution in a hypothetical solvent, which is called vacancy. The vacancy can be understood as the vacuum unit of both phases, which can be filled with adsorbed molecules. If the adsorption equilibrium exists, then the adsorption of a pure gas can be expressed as a two-component equilibrium of adsorbate and vacancy. At equilibrium the chemical potential of the adsorbate is equal to the chemical potential of the gas phase

$$\boldsymbol{\mu_i^s = \mu_{0,i}^s + RTln\left(\gamma_i^s x_i^s\right) + \pi A_{OF,i}^s = \mu_i^g = \mu_{0,i}^g + RTln\left(\gamma_i^g x_i^g\right)}, \qquad (3)$$

with the activity coefficient γ_i, the molar fraction of the adsorbed phase x_i, the spreading pressure π and the surface A_{OF}. Assumption of a pure solution, so that $x_{V,s} = x_{V,g} = 1$ and $\gamma_{V,s} = \gamma_{V,g} = 1$, will lead to equal chemical potentials in the vacancy. By applying this approach to the Gibbs adsorption isotherm equation[10], the isotherm model of the *vacancy solution model* can be expressed as

$$\mathbf{P} = \left(\frac{\mathbf{n_{max}}}{\mathbf{H_{VS}}} \cdot \frac{\boldsymbol{\theta}}{\mathbf{1-\theta}}\right) \cdot \mathbf{f}\left(\boldsymbol{\theta}, \boldsymbol{\gamma}_V^s\right), \qquad (4)$$

with the maximum of adsorbed amount n_{max}, the surface coverage θ, the Henry's law constant H_{VS} and the activity coefficient γ^s_V. The activity coefficients can be further expressed with different approaches. Here, we used the Wilson equation, which was developed to describe vapor-liquid equilibria.[9] Thus, the activity coefficient of the vacancy can then be described by equation (5)

$$\mathbf{ln\gamma_V^s = -ln\left(x_V^s + \Lambda_{V1} \cdot x_1^s\right) - x_1^s \cdot \left(\frac{\Lambda_{1V}}{x_1^s + \Lambda_{1V} \cdot x_V^s} - \frac{\Lambda_{V1}}{x_V^s + \Lambda_{V1} \cdot x_1^s}\right)}. \qquad (5)$$

An overview of models for the description of the activity coefficient in combination with the vacancy solution was given by *Koter et al.*.[14] By Application of equation (5) to equation (4), the isotherm model of the vacancy solution theory in combination with the Wilson equation can be written as

$$P = \left(\frac{n_{max}}{H_{VS}} \cdot \frac{\theta}{1-\theta}\right) \cdot \left(\Lambda_{1V} \cdot \frac{1-(1-\Lambda_{V1})\cdot\theta}{\Lambda_{1V}+(1-\Lambda_{1V})\cdot\theta}\right) \cdot \exp\left(-\frac{\Lambda_{V1}\cdot(1-\Lambda_{V1})\cdot\theta}{1-(1-\Lambda_{V1})\cdot\theta} - \frac{(1-\Lambda_{1V})\cdot\theta}{\Lambda_{1V}+(1-\Lambda_{1V})\cdot\theta}\right). \quad (6)$$

This isotherm equation uses four parameters, the maximum of adsorbed amount n_{max}, the Henry's law constant H_{VS} and the interaction parameters Λ_{1V} und Λ_{V1}.[11]

3.2 Models for the prediction of binary gas adsorption

Ideal adsorbed solution theory

The ideal adsorbed solution theory was published in 1965 by Myers and Prausnitz.[12] The main feature of this model is the possibility of calculating binary adsorption equilibria by using pure component adsorption data. Assumption of an ideal adsorbed phase, which is in equlibrium with a perfect gas phase, leads to activity coefficients equal to 1. Comparison to Raoult's law thus

$$y_i P = P_i^0(\pi)\cdot x_i, \quad (7)$$

with the mixture pressure P, the molar fraction of the gas phase y_i and of the adsorbed phase x_i for component i and the equilibrium gas phase pressure P_i^0 of the pure component i corresponding to temperature and spreading pressure π of the mixture. Assuming the equality of the spreading pressure for each component to the spreading pressure of the mixture, one can write

$$\pi_1^0 = \pi_2^0 \quad (8)$$

and

$$\pi_i^0 = \psi_i\left(P_i^0\right), \quad (9)$$

with the pressure dependent spreading pressure. This dependency can then be expressed by using the Gibbs adsorption isotherm[10] to be

$$\frac{\pi_i^0 \cdot A_{OF}}{RT} = \int_0^{P_i^0} n \cdot d\ln P. \quad (10)$$

The spreading pressure can now be calculated for both pure components i by using a pure gas adsorption isotherm model, which represents the experimental pure gas adsorption data.[10,15] Herein, we used the Tòth isotherm model for this purpose. Thus, by solving equation (7) to (10) simultaneously for given y_i and P, the adsorbed phase molar fraction x_i can be calculated. Subsequently, applying the Lewis rule[16]

$$\frac{1}{n_m^s} = \frac{x_1}{n_1^0} + \frac{x_2}{n_2^0} \tag{11}$$

leads us to the adsorbed amount of both components in gas mixture equilibria.

Vacancy solution model

Based on the pure gas adsorption isotherm equation of the *vacancy solution model*[11], it is possible to predict binary adsorption equilibria. In equilibrium state, the adsorbed phase, the gas phase and the vacancy contains both components 1 and 2. After rearrangement of equation (3), the chemical potential can be written as

$$\varphi_i y_i P = \gamma_i^s x_i^s \cdot \exp\left(\frac{\Delta G_i^0}{RT}\right) \cdot \exp\left(\frac{\pi A_{OF,i}}{RT}\right), \tag{12}$$

with the fugacity coefficient of component i φ_i, the molar fraction of the gas phase y_i and the molar fraction of the adsorbed phase x_i^S of component i and ΔG_i^0 as the free energy or the change of chemical potentials.[13] The spreading pressure π is determined from the equation of state of the adsorbate to

$$-\frac{\pi \cdot \bar{A}_{OF,V}}{RT} = \ln\left(\gamma_i^s x_i^s\right), \tag{13}$$

with the activity coefficient γ^S_i for the three phases of component 1 and 2, and the vacancy and the partial molar area $\bar{A}_{OF,V}$ of the vacancy.[13] Here, the activity coefficients can be obtained from the Wilson equation for a ternary mixture. For the activity coefficients of both components and γ^S_1 and γ^S_2 the Wilson equation can be written as

$$\ln\gamma_i^s = 1 - \ln\left(x_i^s + \Lambda_{i,j} \cdot x_j^s + \Lambda_{i,V} \cdot x_V^s\right) - \left(\frac{x_i^s}{x_i^s + \Lambda_{i,j} \cdot x_j^s + \Lambda_{i,V} \cdot x_V^s} + \frac{\Lambda_{j,i} \cdot x_j^s}{\Lambda_{j,i} \cdot x_i^s + x_j^s + \Lambda_{j,V} \cdot x_V^s} + \frac{\Lambda_{V,i} \cdot x_V^s}{\Lambda_{V,i} \cdot x_i^s + \Lambda_{V,j} \cdot x_j^s + x_V^s}\right), \tag{14}$$

with i, j = 1, 2 or 2, 1 and for the vacancy

$$\ln\gamma_V^s = 1 - \ln\left(\Lambda_{V,i} \cdot x_i^s + \Lambda_{V,j} \cdot x_j^s + x_V^s\right) - \left(\frac{\Lambda_{i,V} \cdot x_i^s}{x_i^s + \Lambda_{i,j} \cdot x_j^s + \Lambda_{i,V} \cdot x_V^s} + \frac{\Lambda_{j,V} \cdot x_j^s}{\Lambda_{j,i} \cdot x_i^s + x_j^s + \Lambda_{j,V} \cdot x_V^s} + \frac{x_V^s}{\Lambda_{V,i} \cdot x_i^s + \Lambda_{V,j} \cdot x_j^s + x_V^s}\right). \tag{15}$$

Furthermore, the saturation loading n^s_{max} of the mixture depends of both pure components to be

$$\mathbf{n^s_{max} = x_1 \cdot n_{max,1} + x_2 \cdot n_{max,2}}\,. \tag{16}$$

To express the relationship for the partial molar area of the adsorbed phase $\bar{A}_{OF,i}$ a special form of Lucassen-Reynders equation of state for homogeneous surfaces is used. This allows the expression of the surface of the vacancy as

$$\mathbf{\overline{A}_{OF,V} = \frac{A_{ges}}{n^s_{max}}} \tag{17}$$

and for both components i by considering of equation (16)

$$\mathbf{\overline{A}_{OF,i} = \overline{A}_{OF,V} + \left(1 - \frac{n_{max,i}}{n^s_{max}}\right) \cdot \frac{A_{ges}}{n^s_m}}, \tag{18}$$

with i = 1,2 and the saturation loading $n_{max,i}$ of pure components i, saturation loading of the mixture n^s_{max} and adsorbed amount of the mixture n^s_m. Substituting of equation (17) and (18) into equation (13) leads to the expression of the spreading pressure of the different phases

$$\mathbf{-\frac{\pi \cdot \overline{A}_{OF,i}}{RT} = \left(1 + \frac{\left(n^s_{max} - n_{max,i}\right)}{n^s_m}\right) \cdot \ln\left(\gamma^s_i x^s_i\right)}. \tag{19}$$

The free energy ΔG_i^0 is given from equation (12) by defining the limit of loading at $P \rightarrow 0$ and adding of the Wilson equation for pure components 1 and 2

$$\mathbf{\exp\left(\frac{\Delta G^0_i}{RT}\right) = \frac{n_{max,i}}{H_{VS,i}} \cdot \Lambda_{i,V} \cdot \exp\left(\Lambda_{V,i} - 1\right)}. \tag{20}$$

Substitution of equation (20) into equation (12) leads to the equilibrium state of the adsorbed phase of component i

$$\mathbf{\varphi_i y_i P = \gamma^s_i x_i n^s_m \cdot \frac{n_{max,i} \cdot \Lambda_{i,V}}{n^s_{max} \cdot H_{VS,i}} \cdot \exp\left(\Lambda_{V,i} - 1\right) \cdot \exp\left(\frac{\pi \overline{A}_{OF,i}}{RT}\right)}. \tag{21}$$

The parameter $n_{max,i}$, $H_{VS,i}$, $\Lambda_{V,i}$ und $\Lambda_{V,i}$ were obtained from the pure gas adsorption isotherm modelling. Additionally, applying

$$\mathbf{x_1 + x_2 = 1} \tag{22}$$

$$\mathbf{y_1 + y_2 = 1} \tag{23}$$

and assuming of an ideal adsorbed phase leads to the final expression for component 1

$$\begin{aligned}\mathbf{\gamma^s_1 x_1 n^s_m \cdot \frac{n_{max,1} \cdot \Lambda_{1,V}}{n^s_{max} \cdot H_{VS,1}} \cdot \exp\left(\Lambda_{V,1} - 1\right) \cdot \exp\left(\frac{\pi \overline{A}_{OF,1}}{RT}\right) =} \\ \mathbf{P - \gamma^s_2 \cdot (1 - x_1) \cdot n^s_m \cdot \frac{n_{max,2} \cdot \Lambda_{2,V}}{n^s_{max} \cdot H_{VS,2}} \cdot \exp\left(\Lambda_{V,2} - 1\right) \cdot \exp\left(\frac{\pi \overline{A}_{OF,2}}{RT}\right)}\end{aligned}. \tag{24}$$

Equation (24) can then be solved for a given adsorbed phase molar fraction x_1 to obtain the adsorbed amount of the mixture n^s_m. Partial loading can afterwards be calculated by applying Lewis rule (equation (11)).[13,16]

3.3 Van Ness method for calculation of partial loading

In case of the gravimetric method only the sum of the adsorbed mass of both components can be measured.[17] The calculation of the partial loading in terms of amount of adsorbate in mmol g^{-1} is not possible from the experimental data given by the gravimetric method.[18] Therefore, the molar fraction and the partial loading of each component has to be calculated by the van Ness method.[17] Basic assumptions are analogous to the IAS theory and include the ideality of the gas phase and the adsorbed phase. With these assumptions, the Gibbs adsorption isotherm for binary mixture can be written as

$$-\left(\frac{\overline{A}_{OF}}{nRT}\right)d\pi + d\ln P + \frac{x_1 - y_1}{y_1 \cdot (1 - y_1)} \cdot dy_1 = 0 . \qquad (25)$$

By adding equation (26)

$$\left(\frac{n}{\overline{A}_{OF}}\right) = \left(\frac{m^{\sigma}_{ges}}{\overline{M}}\right), \qquad (26)$$

and equation (27)

$$\overline{M} = x_1 M_1 + (1 - x_1) M_2 \qquad (27)$$

to equation (25) it is possible to express the experimental measured value of the sum of both components m^{σ}_{ges} as a function of both components. At constant temperature and pressure, after applying equation (10), (26) and (27), equation (25) can be rearranged to calculate the molar fraction of the adsorbed phase x_1 of component 1

$$x_1 = y_1 \cdot \frac{m^{\sigma}_{ges} + (1 - y_1) \cdot M_2 \cdot \left[\frac{\partial\left(\frac{\pi}{RT}\right)}{\partial y_1}\right]_{T,P}}{m^{\sigma}_{ges} + y_1 \cdot (1 - y_1) \cdot (M_2 - M_1) \cdot \left[\frac{\partial\left(\frac{\pi}{RT}\right)}{\partial y_1}\right]_{T,P}} . \qquad (28)$$

Since the average value of the molar mass of adsorbate $\overline{M}$ is a function of the desired molar fraction of the adsorbed phase x_1, equation (28) has to be solved iteratively. Therefore, the spreading pressure of each binary adsorption isotherm and for both pue gas adsorption

isotherms at the same temperature was calculated with the Tòth isotherm model. The dependency of the spreading pressure as a function of the gas phase composition of component 1 in equation (28) was then modelled with a fourth-polynomial function to obtain the molar fraction of the adsorbed phase iteratively. Applying the Lewis rule[16] leads to the partial loading of both components.

4 Volumetric-chromatographic set-up

4.1 Determination of vessel volume

The determination of the volume of the volumetric-chromatographic set-up was carried out by expansion experiments with nitrogen at 298 K and pressures up to 5 MPa. Therefore, the expansion experiments were carried with and without copper filled sample vessel. Copper with a purity of 99.998% was chosen as the filling material because it is chemically inert to nitrogen and has a precisely known density. The basic relation for the calculation of the volume of the set-up is the mass balance (29) of the gasphase

$$\mathbf{m^i = m^j}, \tag{29}$$

where the superscript "i" refers to the mass within the volume V^i before the expansion and the index "j" to the mass within in the volume V^j after the expansion. By combining both expansion experiments with and without copper filled vessels, the mass balance (29) is then transferred to

$$\mathbf{V^i = \frac{\rho_{bulk}^{*,j} \cdot \rho_{bulk}^{j}}{\rho_{bulk}^{j} \cdot \left(\rho_{bulk}^{*,i} - \rho_{bulk}^{*,j}\right) - \rho_{bulk}^{*,i} \cdot \left(\rho_{bulk}^{i} - \rho_{bulk}^{j}\right)} \cdot \left(m_{Cu} \cdot \rho_{bulk}^{j}\right)}. \tag{30}$$

The star symbolises the empty expansion attempt. It should be further noted that according to Equation (31), the mass balance for the required density is always a function of the measured temperature and pressure

$$\mathbf{\rho_{bulk} = \frac{m}{V} = f(P,T)}. \tag{31}$$

The corresponding densities are derived from the pressure and temperature measurements during the expansion series and considering the equation of state for N_2. Therefore, the program *FLUIDCAL* was used.[19] For each volume, given in table SI2, experiments between different volumes and at least ten pressure drop measurements were used to calculate the individual volumes V1 – V6. A detailed description can be found in reference.[20]

Tab. SI2 Parameter of volumetric-chromatographic set-up.

Volume	V / cm^3
volume V1	13.362 ± 0.038
volume V2	18.594 ± 0.052
volume V3	10.030 ± 0.028
volume V4	5.481 ± 0.015
volume V5	11.438 ± 0.032
volume V6	1.170 ± 0.003
total volume	60.075 ± 0.169

4.2 Validation of volumetric-chromatographic set-up

For a validation of the newly established volumetric-chromatographic apparatus, an extensively studied adsorbate/adsorbent system was chosen. On this account, the adsorption of CO_2 on the microporous activated carbon Norit R1 Extra was carried out at 298 K. In Figure S4 the CO_2 and CH_4 adsorption isotherms are shown. Up to a pressure of 2 MPa, a very good agreement with the reference data occur. At higher pressures, there are significant differences between the isotherms compared to the literature data. This might be due to the inhomogeneity of the activated carbon. *Dreisbach*[21,22] used activated carbon with an inner surface of 1407 – 1419 m^2 g^{-1}, while *Beutekamp*[23,24], *Herbst*[25,26] and *Bazan*[27] published surfaces of around 1260 - 1300 m^2 g^{-1}. However, the loadings of carbon dioxide given by *Dreisbach*[21,22] are the lowest at this comparison. The activated carbon used in this study consists of an internal surface area of 1332 m^2 g^{-1}. The micropore volumes of all activated carbon samples are nearly identical in the range of 0.60 ± 0.02 cm^3 g^{-1}. Another possible reason for the deviation at high pressures is the fact that the specific sample volumes $V_{spez.,He}$, calculated from He measurements differ slightly. Thus, the specific sample volume varies between $V_{spez.,He}$ = 0.351 cm^3 g^{-1} (*Dreisbach*[21,22]) to 0.459 cm^3 g^{-1} (*Bazan*[27]) and 0.462 cm^3 g^{-1} (*Beutekamp*[24] and *Herbst*[26]). Whereas, in this study the specific sample volume was determined to be $V_{spez.,He}$ = 0.476 cm^3 g^{-1}. The difference in internal surface and sample volume support the occurrence of the inhomogeneous nature of the activated carbon Norit R1 Extra.

In addition to the validation by pure gas adsorption, binary adsorption equilibria of an equimolar mixture of CO_2 and CH_4 were measured at 298 K and pressures of 0.1 MPa and 1 MPa on activated carbon Norit R1 Extra. By applying the IAS theory and the single component Tòth isotherm model, partial and total loadings of the adsorbate/adsorbent -system

was predicted. The comparison, shown in Figure SI5 and Figure SI6, clarify the good agreement between the experimental data and the prediction by IAS theory. Moreover, with respect to the reference data by *Beutekamp*[24], *Bazan*[27] and *Dreisbach*[21,22] the adsorbate/adsorbent-system can be considered as an ideal system up to 1 MPa.

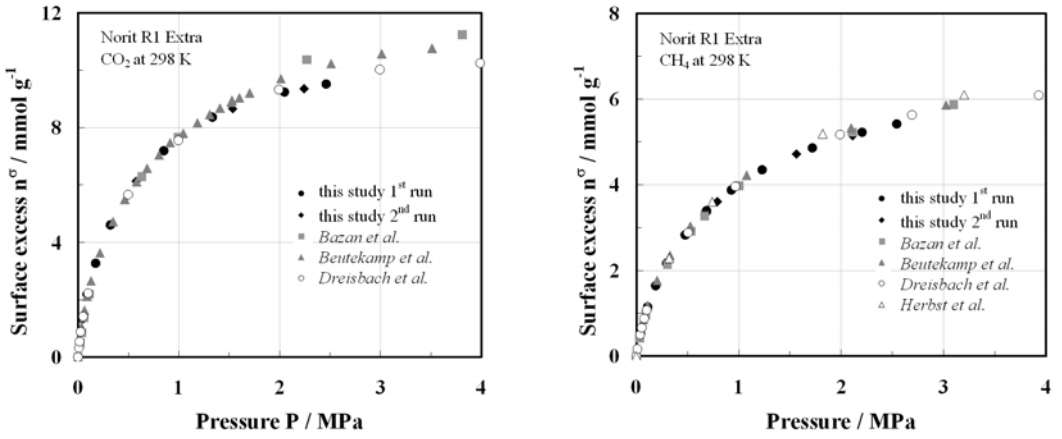

Fig. SI4 CO_2 (left hand side) and CH_4 (right hand side) adsorption isotherms at 298 K on activated carbon Norit R1 Extra.

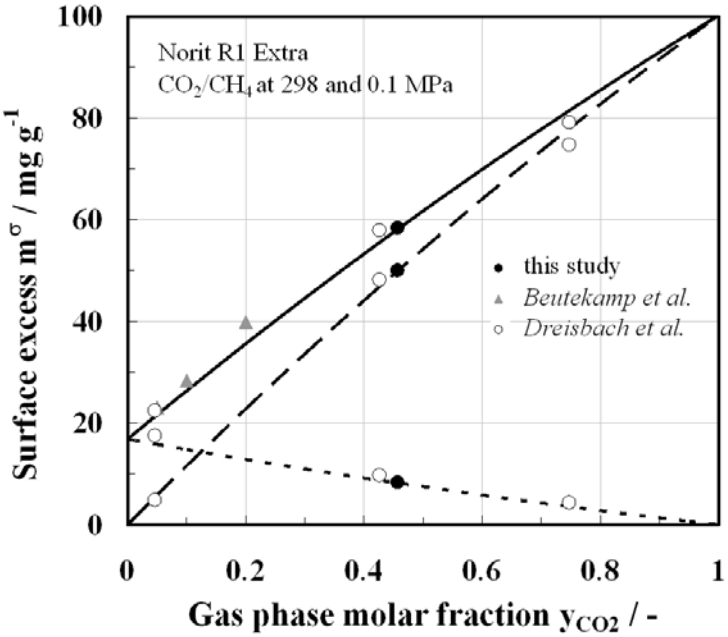

Fig. SI5 CO_2/CH_4 gas mixture adsorption at 298 K and 0.1 MPa on activated carbon Norit R1 Extra (*Beutekamp*[24] by gravimetric method, *Dreisbach*[21,22] by volumetric-chromatographic method; solid lines: IAST + Tòth isotherm model prediction for total adsorbed amount, dotted lines: partial loading of CH_4, dashed lines: partial loading of CO_2).

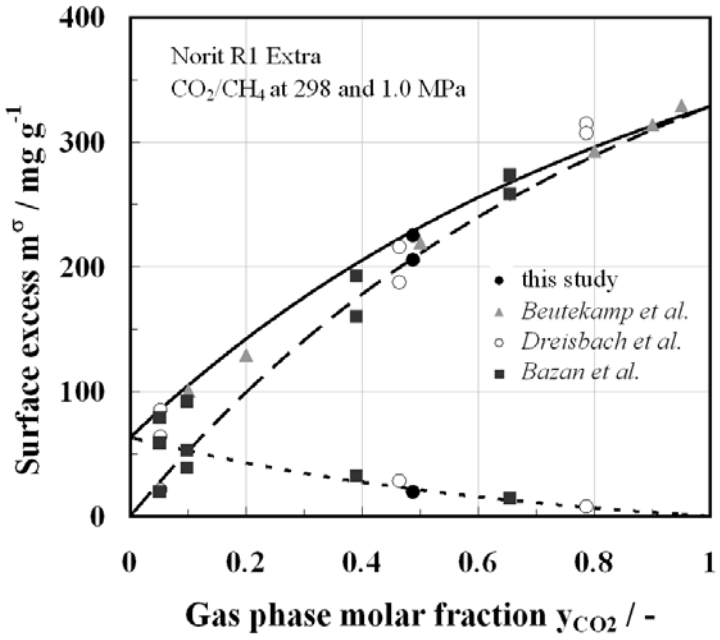

Fig. SI6 CO_2/CH_4 gas mixture adsorption at 298 K and 1.0 MPa on activated carbon Norit R1 Extra (*Bazan*[27] by volumetric-chromatographic method, *Beutekamp*[24] by gravimetric method, *Dreisbach*[21,22] by volumetric-chromatographic method; solid lines: IAST + Tòth isotherm model prediction for total adsorbed amount, dotted lines: partial loading of CH_4, dashed lines: partial loading of CO_2).

5 Binary adsorption of CH_4 and N_2

5.1 Data correlation

The experimental data were modelled with pure gas isotherm model, e.g. the Tòth model and the *vacancy solution model* (VSM). The quality value was set to be the mean relative deviations of the measured values D_n between the experimental values of n^σ and the calculated values for each adsorbate n_{model}. This deviations were calculated by

$$D_n = \frac{100}{k} \cdot \sum_{i=1}^{k} \left| \frac{\left(n^\sigma - n_{model}\right)}{n^\sigma} \right|, \qquad (32)$$

with k as the overall number data points.

For binary adsorption experiments, the same procedure was used for the partial molar loadings n_i and for the adsorbed amount in mass units m_i between experimental data and prediction by IAS theory and VSM to be

$$D_{n,i} = \frac{100}{k} \cdot \sum_{i=1}^{k} \left| \frac{\left(n_i^\sigma - n_{model,i}\right)}{n_i^\sigma} \right| \qquad (33)$$

and

$$D_{m,i} = \frac{100}{k} \cdot \sum_{i=1}^{k} \left| \frac{\left(m_i^{\sigma} - m_{model,i}\right)}{m_i^{\sigma}} \right| . \qquad (34)$$

In analogy to that, derivations between experimental gas phase composition and model predictions were estimated by

$$D_{x,i} = \frac{100}{k} \cdot \sum_{i=1}^{k} \left| \frac{\left(x_i^{\sigma} - x_{,model,i}\right)}{x_i^{\sigma}} \right| . \qquad (35)$$

Tab. SI3 Mean relative deviations between experimental data and modeling by Tòth isotherm equation for binary mixtures of CH_4/N_2 on $_{\infty}^{3}$[Cu(Me-*4*py-trz-ia)] 1 and Basolite®A100.

$_{\infty}^{3}$[Cu(Me-*4*py-trz-ia)] 1	$D_{m,ges}$ / % y_{CH4} = 0.089	$D_{m,ges}$ / % y_{CH4} = 0.175	$D_{m,ges}$ / % y_{CH4} = 0.343	$D_{m,ges}$ / % y_{CH4} = 0.545	$D_{m,ges}$ / % y_{CH4} = 0.763	$D_{m,ges}$ / % y_{CH4} = 0.872
273 K	-	2.25	-	1.71	1.87	-
298 K	0.99	0.29	2.21	1.63	1.00	0.55
323 K	-	0.30	1.77	0.60	1.58	1.94
Basolite® A100	**$D_{m,ges}$ / % y_{CH4} = 0.085**	**-**	**-**	**$D_{m,ges}$ / % y_{CH4} = 0.535**	**$D_{m,ges}$ / % y_{CH4} = 0.755**	**$D_{m,ges}$ / % y_{CH4} = 0.866**
273 K	-	-	-	0.48	0.63	0.51
298 K	1.12	-	-	1.65	1.42	0.89
323 K	-	-	-	1.08	0.55	1.40

5.2 Spreading pressure diagrams

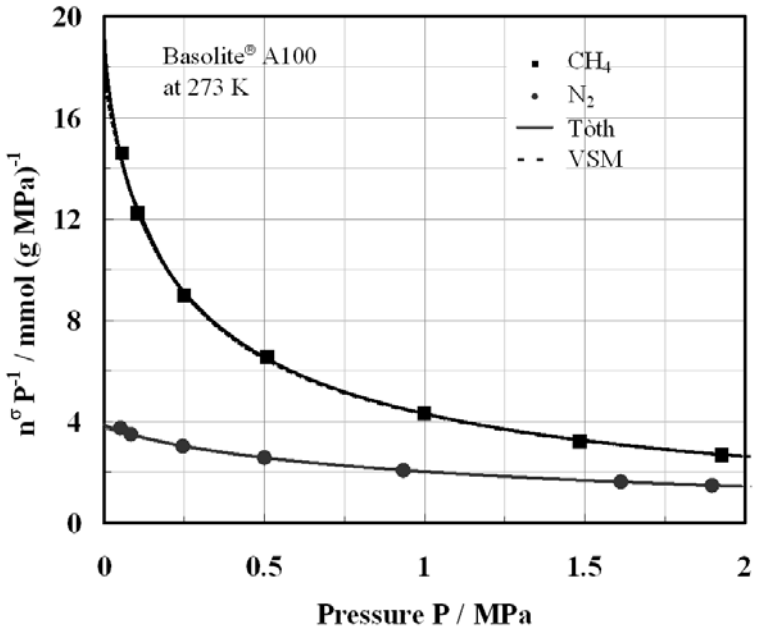

Fig. SI7 **Plot of $n^{\sigma} \cdot P^{-1}$ as a function of pressure for CH_4 and N_2 adsorption on Basolite® A100 at 273 K (solid lines: Tòth isotherm model, dotted lines: VSM).**

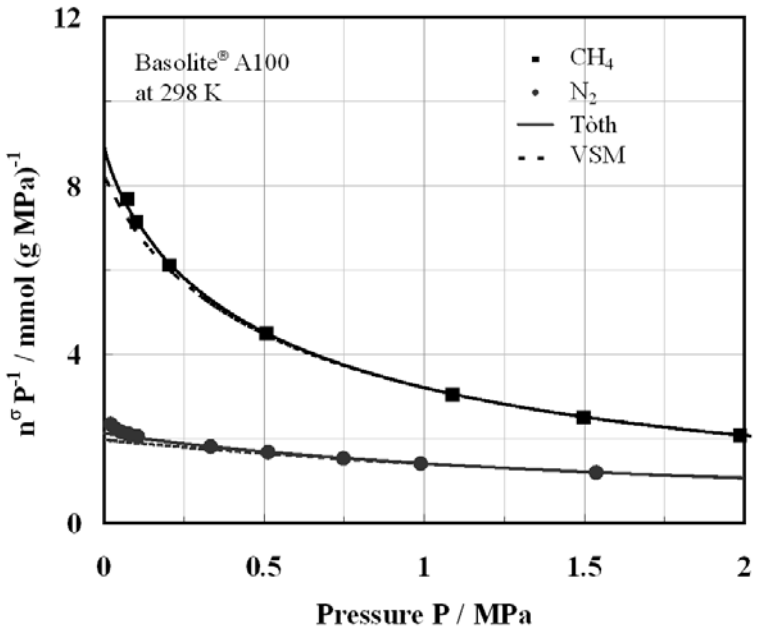

Fig. SI8 **Plot of $n^{\sigma} \cdot P^{-1}$ as a function of pressure for CH_4 (!) and N_2 (#) adsorption on Basolite® A100 at 298 K (solid lines: Tòth isotherm model, dotted lines: VSM).**

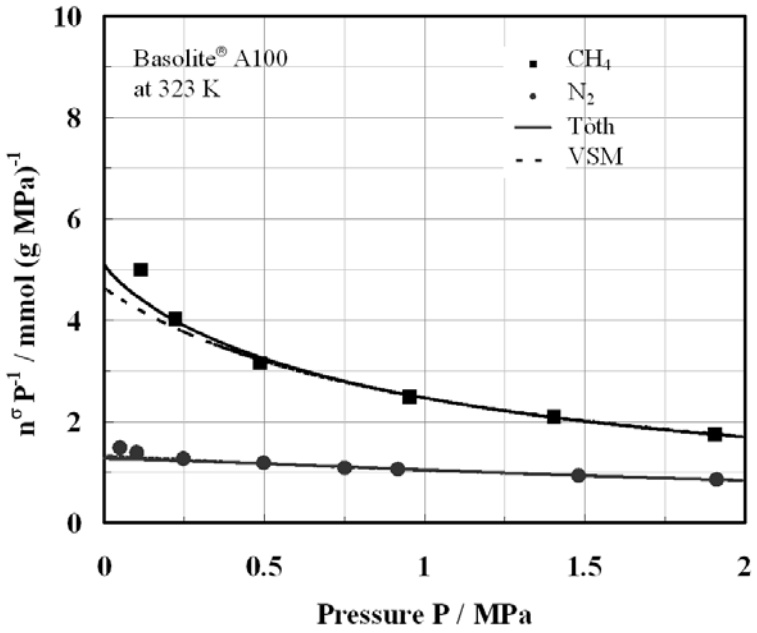

Fig. SI9 Plot of $n^{\sigma}\cdot P^{-1}$ as a function of pressure for CH_4 (!) and N_2 (#) adsorption on Basolite® A100 at 323 K (solid lines: Tòth isotherm model, dotted lines: VSM).

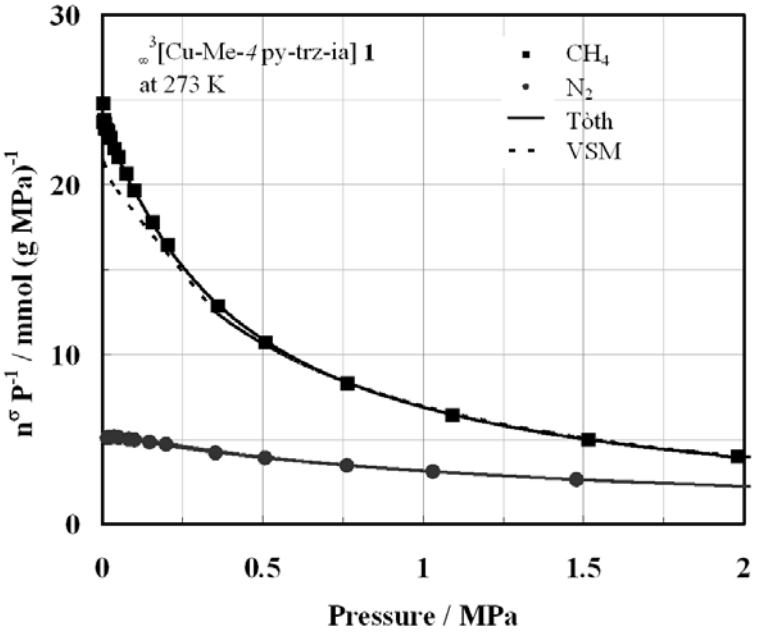

Fig. SI10 Plot of $n^{\sigma}\cdot P^{-1}$ as a function of pressure for CH_4 and N_2 adsorption on $_{\infty}^{3}$[Cu(Me-4py-trz-ia)] 1 at 273 K (solid lines: Tòth isotherm model, dotted lines: VSM).

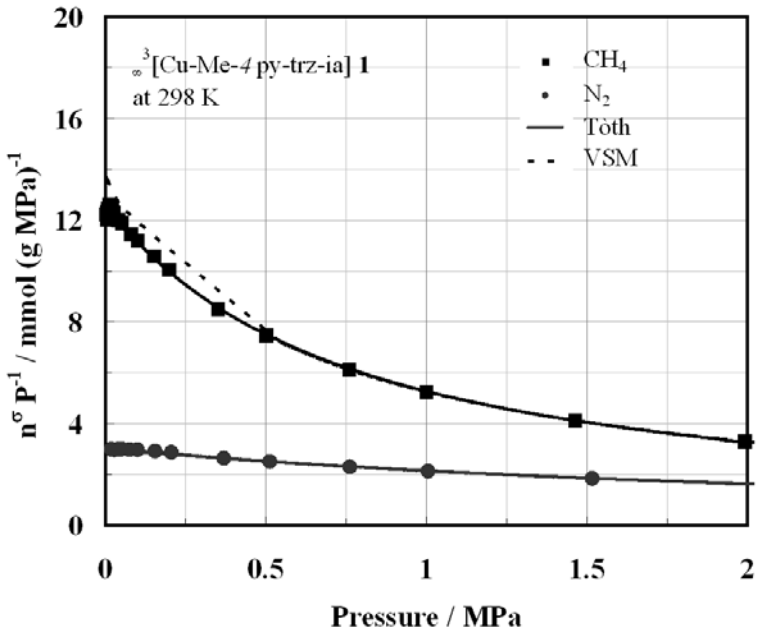

Fig. SI11 Plot of $n^\sigma \cdot P^{-1}$ as a function of pressure for CH_4 and N_2 adsorption on $_\infty^3$[Cu(Me-*4*py-trz-ia)] 1 at 298 K (solid lines: Tòth isotherm model, dotted lines: VSM).

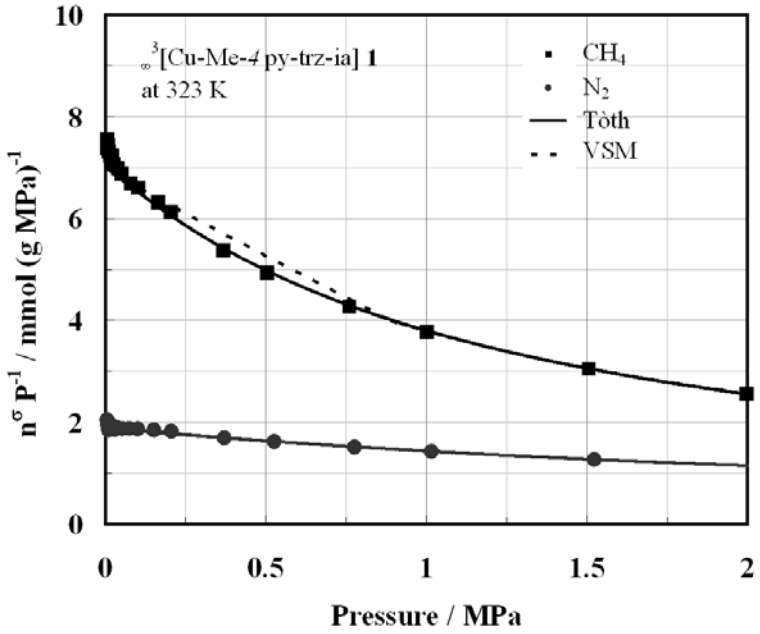

Fig. SI12 Plot of $n^\sigma \cdot P^{-1}$ as a function of pressure for CH_4 and N_2 adsorption on $_\infty^3$[Cu(Me-*4*py-trz-ia)] 1 at 323 K (solid lines: Tòth isotherm model, dotted lines: VSM).

5.3 McCabe-Thiele Plots

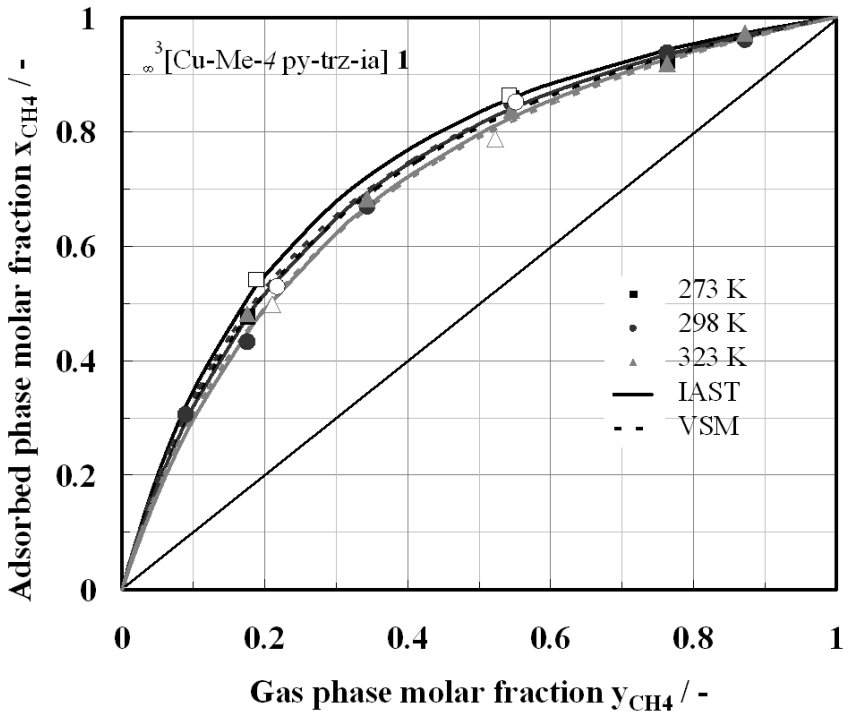

Fig. SI13 **McCabe-Thiele-Plots for binary adsorption of CH_4 and N_2 on $_\infty^3$[Cu(Me-*4*py-trz-ia)] 1 at 273 K, 298 K and 323 K and 0.5 MPa (solid lines: IAST + Tòth isotherm model, dotted lines: VSM; closed symbols by gravimetric method and applying van Ness procedure, open symbols from volumetric-chromatographic method).**

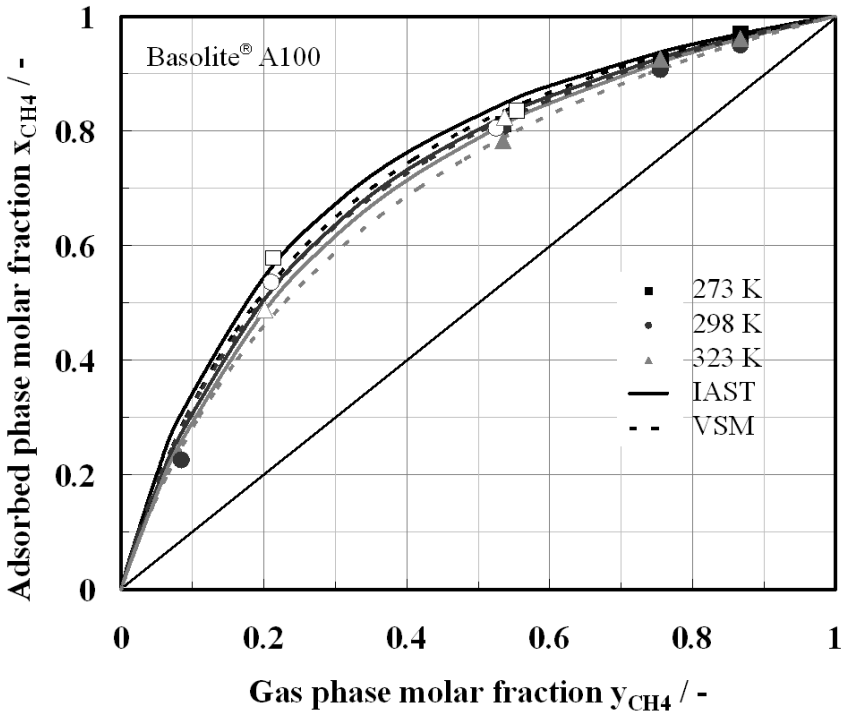

Fig. SI14 **McCabe-Thiele-Plots for binary adsorption of CH_4 and N_2 on Basolite© A100 at 273 K, 298 K and 323 K and 0.5 MPa (solid lines: IAST + Tòth isotherm model, dotted lines: VSM; closed symbols by gravimetric method and applying van Ness procedure, open symbols by volumetric-chromatographic method).**

5.4 Selectivities

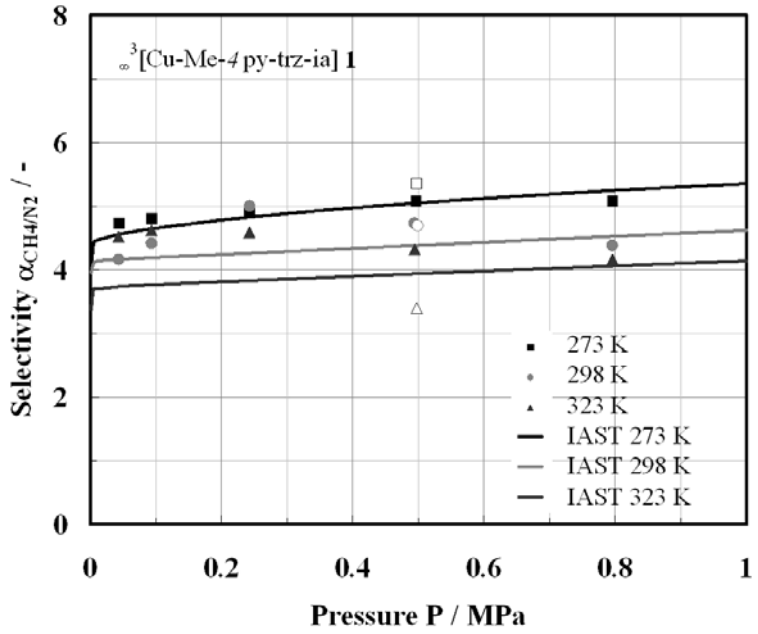

Fig. SI15 **Selectivity of CH_4 from nearly equimolar CH_4/N_2 mixture (y_{CH4} = 0.545) as a function of pressure during adsorption on $_\infty^3$[Cu(Me-4py-trz-ia)] 1 at 273 K, 298 K and 323 K (solid lines: IAST + Tòth isothem model; closed symbols by gravimetric method and applying van Ness procedure, open symbols by volumetric-chromatographic method).**

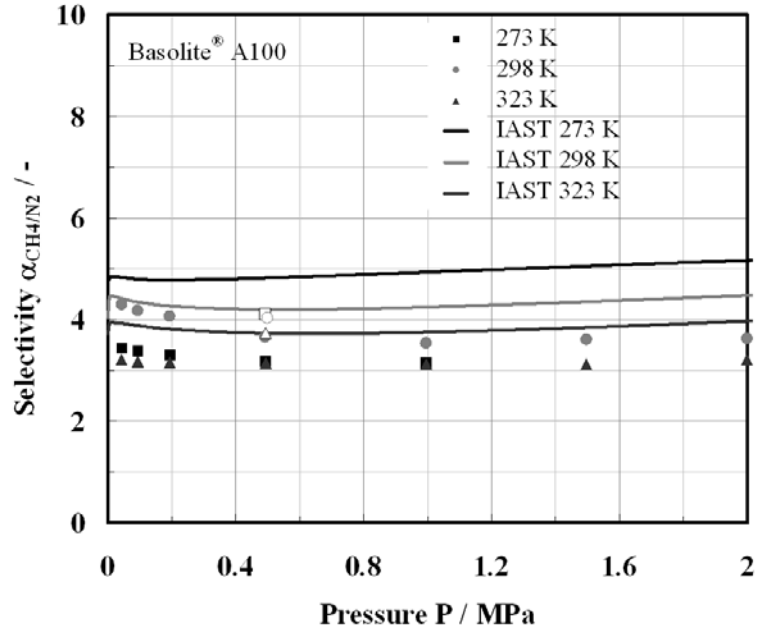

Fig. SI16 **Selectivity of CH_4 from nearly equimolar CH_4/N_2 mixture (y_{CH4} = 0.535) as a function of pressure during adsorption on Basolite®A100 at 273 K, 298 K and 323 K (solid lines: IAST + Tòth isotherm model; closed symbols by gravimetric method and applying van Ness procedure, open symbols by volumetric-chromatographic method).**

6 Notes and References

1 J. Rouquerol, P. Llewellyn and F. Rouquerol, *Stud. Surf. Sci. Catal.* 2007, **106**, 49.

2 ISO/FDIS 9277:2010 – "*Determination of the specific surface area of solids by gas adsorption -- BET method*"

3 J. Moellmer, E.B. Celer, R. Luebke, A.J. Cairns, R. Staudt, M. Eddaoudi and M. Thommes, *Micropor. Mesopor. Materials*, 2010, **129**, 345.

4 L. Gurvich, *J. Phys. Chem. Soc. Russ.* 1915, **47**, 805.

5 S. Lowell, J. Shields, M.A. Thomas and M. Thommes, Characterization of Porous Solids and Powders: Surface Area, Pore Size and Density, Springer, The Netherlands, 2004.

6 BASF-Basolite®-Handout-051908, given by *Sigma Aldrich* homepage http://www.sigmaaldrich.com

7 Data from Cambridge structural database (CSD); www.ccdc.cam.ac.uk.

8 D. Lässig, J. Lincke, J. Moellmer, C. Reichenbach, A. Moeller, R. Glaeser, G. Kalies, K.A. Cychosz, M. Thommes, R. Staudt and H. Krautscheid, *Angew. Chem. Int. Ed.* 2011, **50**, 10344 and *Angew. Chem.* 2011, **123**, 10528.

9 J. Tòth, *Adv. Coll. Inter. Sci.* 1995, **55**, 1.

10 D.D. Do, Adsorption Analysis: Equilibria and Kinetics, Imperial College Press, UK, 1998.

11 S. Suwanayen and R.P. Danner, *AIChE J.* 1980, **26**, 68.

12 A.L. Myers and J.M. Prausnitz, *AIChE J.* 1965, **11**, 121.

13 S. Suwanayen and R.P. Danner, *AIChE J.* 1980, **26**, 76.

14 S. Koter and A.P. Terzyk, *J. Colloid Interface Sci.* 2005, **282**, 335.

15 O. Talu and A. Myers, *AIChE J.* 1988, **34**, 1887.

16 W.K. Lewis, E.R. Gilliland, B. Chertow and W.P. Cadogan, *Ind. Eng. Chem.* 1950, **42**, 1319.

17 H.C. van Ness, *Ind. Eng. Chem. Fundamen.*, 1969, **8**, 464.

18 a) A.L. Myers, *Pure Appl. Chem.* 1989, **61**, 1949; b) E. Buss, *Gas Sep Purif.* 1995, **9**, 189; c) S. Beutekamp and P. Harting, *Adsorption*, 2002, **8**, 255; d) A. Herbst, S. Beutekamp, P. Harting and R. Staudt, *Chem. Ing. Tech.* 2002, **74**, 1405.

19 R. Span, E.W. Lemmon, R.T. Jacobsen, W. Wagner and A. Yokozeki, *J. Phys. Chem. Ref. Data* 2000, **29**, 1361.

20 J.U. Keller, R. Staudt, Gas Adsorption Equilibria, Experimental Methods and Adsorption Isotherms, Springer, New York, USA, 2004.

21 F. Dreisbach, R. Staudt, J.U. Keller, *Adsorption*, 1999, **5**, 215.

22 F. Dreisbach, Ph.D. Thesis, „Untersuchung von Adsorptionsgleichgewichten methanhaltiger Gasgemische an Aktivkohle als Grundlage zur Auslegung technischer Prozesse“, Fortschritt-Berichte VDI-Verlag, 1998.

23 S. Beutekamp, P. Harting, *Adsorption*, 2002, **8**, 255.

24 S. Beutekamp, Ph.D. Thesis, „Adsorptionsgleichgewichte der reinen Gase Methan, Kohlendioxid, Stickstoff und deren binärer Gemische an verschiedenartigen porösen Stoffen“, University of Leipzig, 2001.

25 A. Herbst, P. Harting, *Adsorption*, 2002, **8**, 111.

26 A, Herbst, Ph.D. Thesis, „Exzessadsorption reiner Gase im Druckbereich bis 50 MPa“, University of Leipzig, 2002.

27 R.E. Bazan, Ph.D. Thesis, „Adsorptionsuntersuchungen von methanhaltigen Gasgemischen an Aktivkohle Norit R1“, University of Leipzig, 2010.